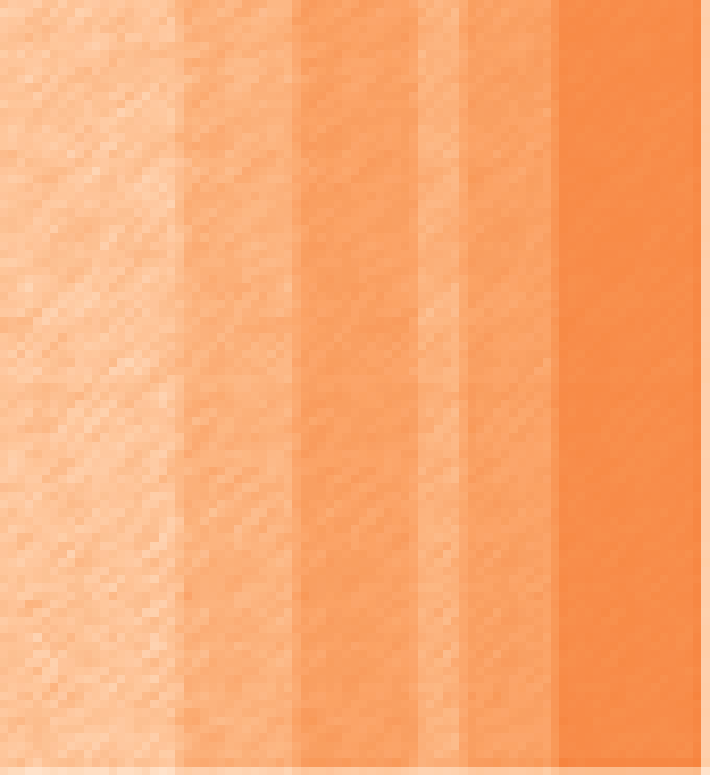

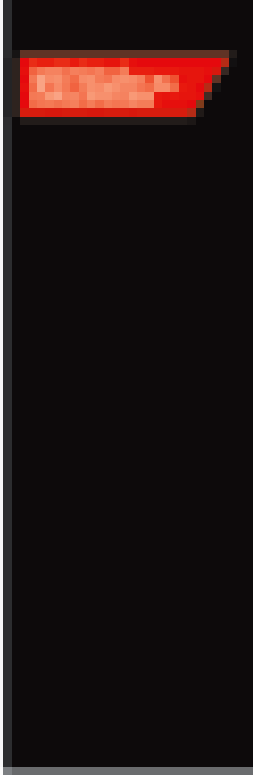

JOURNAL OF

RAIL AND RAPID TRANSIT

The Journal for Railway Engineering

Proceedings of the Institution of Mechanical Engineers
Part F

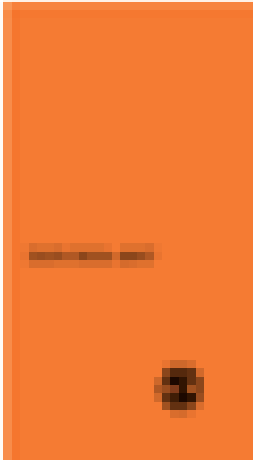

Designing of railway wheels - Part 1. Finite element method

M. Sitarz, A. Sładkowski, K. Bizoń, K. Chruzik
Department of Railway Engineering, Silesian University of Technology, European Centre of Excellence, Poland

Abstract: At present, the design process can be simplified and accelerated, if computer simulation basing on finite element method (FEM) is used. FEM numerical calculations of different wheels of railway wheelsets are investigated in Department of Railway Engineering. The justification for undertaking this issue is that the methodology of design of railway wheelsets both in Poland and abroad is absent; there is no possibility of optimising wheelsets' construction characteristics depending on manufacturing process and service parameters. The analysis of this problem has made possible:

- comparison of software used so far in strain calculation of railway wheelsets;
- elaboration of design methodology for railway wheelsets;
- increase in durability of railway wheelsets;
- increase in the safety of rail transport;
- decrease in manufacturing and service costs of railway wheelsets.

Keywords: finite elements method, numerical analysis, wheelsets, static loads, dynamic loads, thermal loads, stress, deformation

NOTATION

c	coefficient
c_1	coefficient
D	coefficient
E	Young's modulus
h	mesh thickness
$M(r)$	bending moment
P	force
r_1	inner radius of mesh a wheel
r_2	outer radius of mesh a wheel
T	pressing force
T_r	coefficient
$w(r)$	displacements distribution
$\sigma_{r\max}$	maximum strain in radial direction
μ	Lame coefficient
Δ_y	pre-set displacement in y direction
Δ_z	pre-set displacement in z direction
κ	Lame coefficient
ν	Poisson's ratio
$\tau_{r\phi\max}$	maximum strain in circumferential direction
ς	torsion of inner contour
$\Delta\vartheta$	torsion length in circumferential direction
σ_r	strain in radial direction
η	coefficient
μ	friction coefficient

Abbreviations

UIC International Union of Railways

1. INTRODUCTION

In spite of growing competitiveness of the road transport, the rail transport is still the principal long-distance transport system. In some countries (France, UK, Germany) the rail transport experiences its renaissance in city agglomerations (trams, rail bus, metro) and in long-distance travel (high-speed trains). Increased service demands as well as environmental and traffic safety requirements set on rail vehicles in the majority of European states explain the necessity of manufacturing rolling stock fulfilling high quality standards. The modern trains should be faster, cheaper and safer. The travel conditions, i.e. passengers' comfort, should also be improved. All these factors depend most of all on the design of rail vehicle.

The demands set on fast modern rail vehicles and their parts, including the railway wheelsets, can be enumerated as follows [1,2]:

- decreasing weight;
- increasing vehicle elements mechanical strength;
- lessening the noise and vibrations level;
- increasing travel comfort;
- decreasing dynamical interaction between vehicle and the track.

The development of computers and software provides possibilities of modelling new designs of different structural elements of rail vehicles. The phenomena occurring during the vehicle service can be adequately described, The error generated during design or prototype tests can lead to tragic occurrences during the service itself. These may be related to additional financial outlay and lengthening the prototype testing time, but they may also cause incalculable loss of human health or life.

According to the experts, the rail transport is one of the most ecological (Table 1) and safe (Table 2) means of transport. Still, accidents happen [3]. They are not very frequent, but they are highlighted by the media. The most famous accident to date happened in Eschede, Germany, on 3rd June, 1998. Incorrectly designed railway wheelset has caused a tragic derailment and death of 101 persons (Fig.1 [4]). Similar, though less tragic accidents happened lately all over Europe [3]: Rickerscote, 8 March 1996, Sandy, 17 June 1998, Hatfield, 17 October 2000, Potters Bar, 10 May 2002.

Table 1. Comparison of different means of transport

Transport means	Energy consumption in kcal/passenger-km	Carbon dioxide emission in g of carbon /passenger-km
Car	642	45
Bus	196	19
Train	106	5
Airplane	393	30

Table 2. Mortality of the passengers per a hundred million

Transport means	Kilometres	Travels	Hours
Car	0,31	4	13
Bus	0,06	0,5	1
Train	0,08	2	4
Airplane	0,009	20	5

Fig. 1. Derailment of train in Germany - Eschede, 3 June 1998

The advancement in the computers computational speed and the elaboration of complex software based on finite element method (FEM) and devoted to the railway industry demands, results in running calculations and simulations, which have not been previously possible.

There are many issues, which so far have been only experimentally/analytically investigated. The use of numerical methods limits or wholly eliminates the need for some tests or calculations.

The investigation time is therefore decreased, the complex test stands can be replaced with suitable software; hence, financial advantages are gained.

On the basis of the above analysis related to state-of-the-art in the railway wheelsets subject matter, conclusion may be drawn that computation by numerical methods might play significant role in each of the above issues.

It is certain that numerical calculations should be the starting point in the design, assembly and service stress analysis and thermal analysis of the material.

However, the numerical methods are saddled with errors due to the imperfect transformation of the real model into the virtual model. Still, if the investigation methods are used jointly, i.e. experimental tests are backed by numerical analysis, the results obtained may be close to reality.

Basing on the references, the present state-of-the-art of the numerical calculations of the railway wheelset wheels can be summarised as follows:

- lack of universally accepted computational algorithm of railway wheels,
- inadequate experimental confirmation of the correctness of computational procedures used at present,
- absence of comparison of numerical calculations of railway wheels done with the help of different software,
- discrepancies in set boundary conditions,
- absence of precise algorithm for creating FEM model for railway wheels (type, distribution and size of element)

- complexity of stress calculation method, when the stress is due to assembly-time interference,
- lack of UIC certification for calculations of thermal stress due to braking.

2. NUMERICAL ANALYSIS OF THE WHEELSETS' WHEELS

The railway wheelset is a constructional element influencing directly the vehicle motion as well as passengers' safety. That is why the axle, wheel and the wheelset itself must be characterised by adequate mechanical strength during the service period. Nowadays the railway wheelsets designs used are the effect of service experience and process engineering. Lately, the numerical analyses of stress and strain done in the wheelset design phase are also utilised.

At present, the design process can be simplified and accelerated, if computer simulation basing on finite element method (FEM) is used. FEM numerical calculations of different wheels of railway wheelsets are investigated in Department of Railway Engineering. Three software packages are used – ANSYS, NASTRAN and COSMOS. This diversity of software should make possible the comparison of convergence of results (tolerance, computation time), provided that input data are identical (e.g. wheel geometry, material. boundary conditions, FEM mesh). Before the calculations are started, these data must be established, if the results are to be comparable.

The justification for undertaking this issue is that the methodology of design of railway wheelsets both in Poland and abroad is absent; there is no possibility of optimising wheelsets' construction characteristics depending on manufacturing process and service parameters. The analysis of this problem has made possible:

- comparison of software used so far in strain calculation of railway wheelsets;
- elaboration of design methodology for railway wheelsets;
- increase in durability of railway wheelsets;
- increase in the safety of rail transport;
- decrease in manufacturing and service costs of railway wheelsets.

2.1. Initial investigations – mesh of a wheel model

In order to make FEM calculations more accurate, the comparison of analytical and numerical methods of calculations has been conducted on the basis of mesh of a wheel model. Figure 2 shows the mesh of a wheel model and physical and discrete models generated by the software

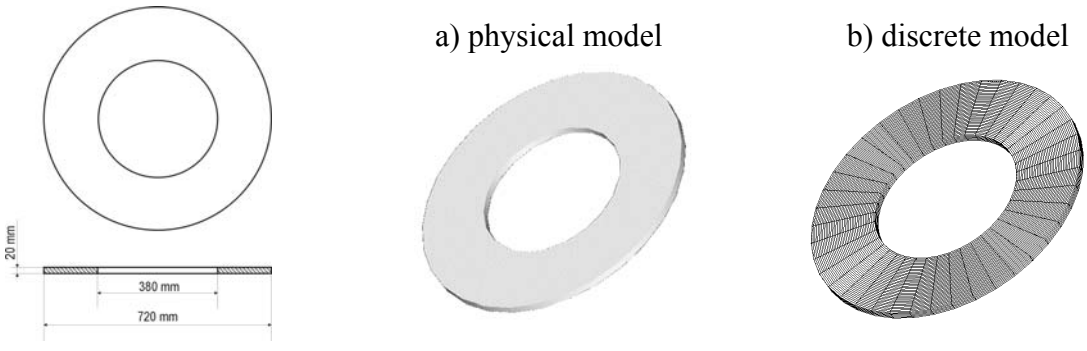

Fig. 2. Model of the mesh of a wheel

Three possible loads have been considered – see Fig.3. In case of the first load, the initial displacements of the nodes of inner surface generator parallel to y-axis of the global Cartesian co-ordinate system have been defined (Fig. 3.a). In the case of second load, the initial displacement of the nodes has been alongside T-angle of polar co-ordinate system – Fig. 3.b. In the case of third load, the nodes have been linearly displaced parallel to the z-axis of Cartesian co-ordinate system – Fig.3.c. The maximum strains for the presented loads have been calculated analytically. The data: mesh thickness h = 0,02 [m], inner radius outline r_1 = 0,019 [m] and outer radius r_2= 0,36 [mm] [5]:

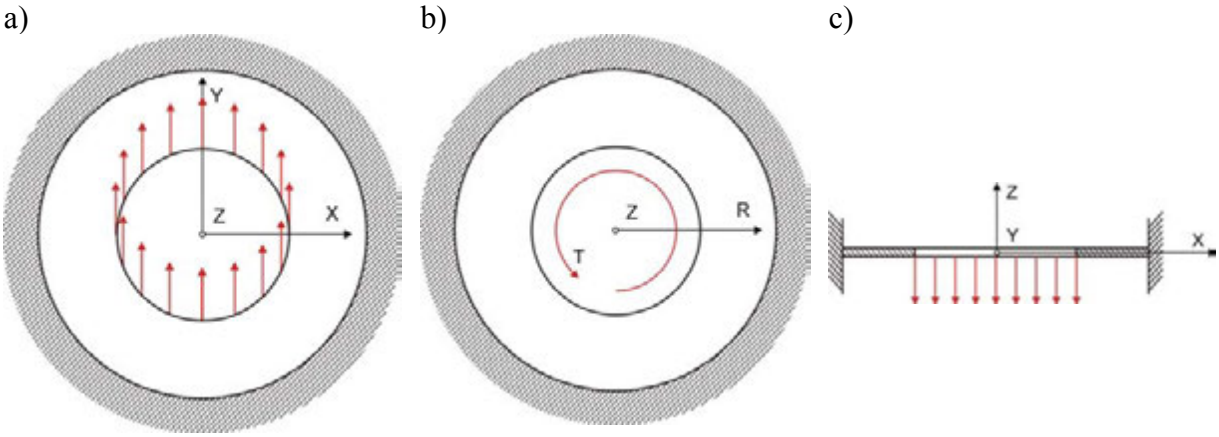

Fig. 3. Load models for the mesh a wheel

Case # 1.

$$\sigma_{r\max} = \frac{\mu \cdot \Delta_y}{c}\left[\frac{3 \cdot \kappa\left(r_1^2 + r_2^2\right)}{r_1} + 2r_1 + \frac{\kappa^2\left(r_1^2 + r_2^2\right)}{r_1} - 2\frac{\kappa r_2^2}{r_1}\right] \tag{3.1.}$$

where μ and κ are Lame coefficients, calculated from the formulas:

$$\mu = \frac{E}{2(1+\nu)}$$
$$\kappa = \frac{3-\nu}{1+\nu} \tag{3. 2.}$$

E – Young's modulus

ν –Poisson's constant

Δy – pre-set displacement = 0,0001 [m]

Coefficient c has been determined with the help of formula:

$$c = r_1^2 - r_2^2 - \kappa^2(r_1^2 + r_2^2)\ln\frac{r_1}{r_2} \tag{3. 3.}$$

For this equation

$$\sigma_{r\max} = 143{,}9\ \text{MPa} \tag{3. 4.}$$

Case # 2

$$\tau_{r\phi max} = \frac{2 \cdot \mu \cdot r_1^2 \cdot \varsigma}{r_2^2 - r_1^2} \tag{3. 5.}$$

where ς - torsion of inner contour, torsion angle is

$$\varsigma = \frac{\Delta\vartheta}{r_1} \tag{3. 6.}$$

for $\Delta\vartheta = 0{,}0001$ [m]

$$\tau_{r\phi max} = 110{,}5 \text{ MPa} \tag{3. 7.}$$

Case # 3

$$\sigma_r = 6\frac{M(r)}{h^2} \tag{3. 8.}$$

where bending moment at mesh cross-section, derived from formula:

$$M(r) = D\left[\frac{d^2}{dr^2}w(r) + \frac{\nu}{r}\frac{d}{dr}w(r)\right] \tag{3. 9.}$$

depends on the displacements distribution of the mesh

$$w(r) = \frac{T_r r_2}{8\pi D(\eta^2 - 1)}\left\{\left[\ln(\eta) - 1 + \frac{\eta^2 + 1}{2}\right]\left(1 - \frac{r_1^2}{r_2^2}\right) - \left[2\ln(\eta) + (\eta^2 - 1)\frac{r_1^2}{r_2^2}\right]\ln\left(\frac{r_2}{r_1}\right)\right\} \tag{3. 10.}$$

Bending rigidity and axial forces have been calculated from the formulas:

$$D = \frac{Eh^3}{12(1 - \nu^2)}$$

$$T_r = \frac{\Delta z}{c_1}$$

$$c_1 = \frac{\left[\ln(\eta) - 1 + \frac{\eta^2 + 1}{2}\right]\left(1 - \frac{r_1^2}{r_2^2}\right) - \left[2\ln(\eta) + (\eta^2 - 1)\frac{r_1^2}{r_2^2}\right]\ln\left(\frac{r_2}{r_1}\right)}{8\pi D(\eta^2 - 1)} r_2 \tag{3. 11.}$$

$$\eta = \frac{r_2}{r_1}$$

$$\sigma_{r max} = 60{,}5 \text{ MPa} \tag{3. 12.}$$

At the same time, meshes have been generated, differing one from the other by the size and distribution of elements as well as the type of element used.

The investigation has resulted in determination of the percentage error of numerical analysis, which depends on the size and distribution of the elements and on type of element used.

Figure 4a illustrates graphically the computation error for the third and most typical load; computation time is shown in Fig.4b.

a)

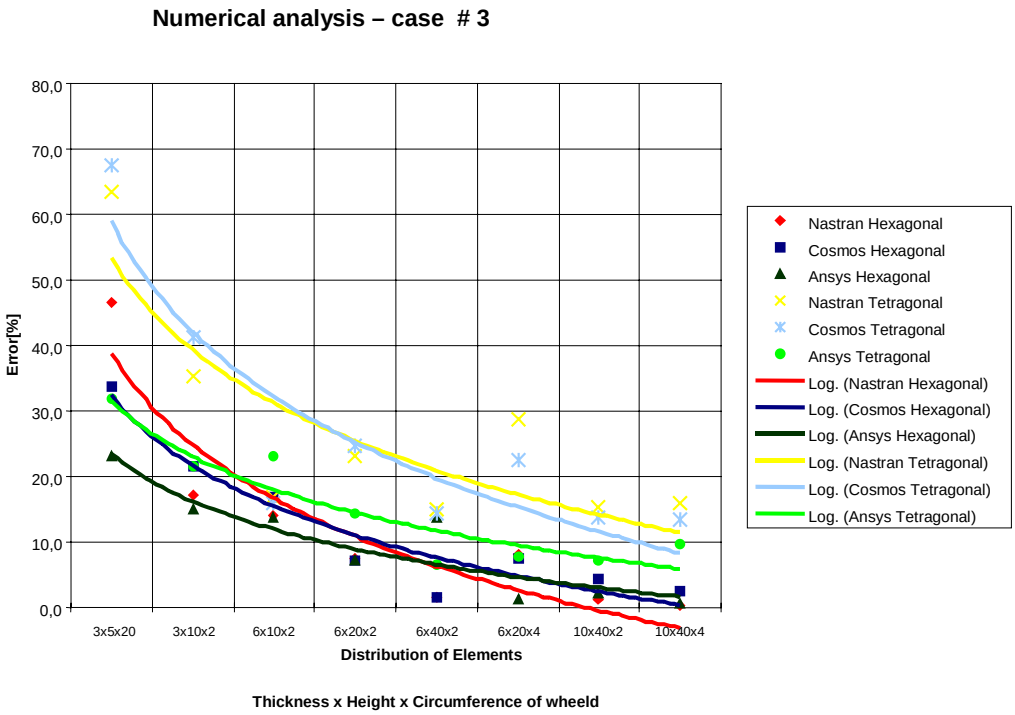

b)

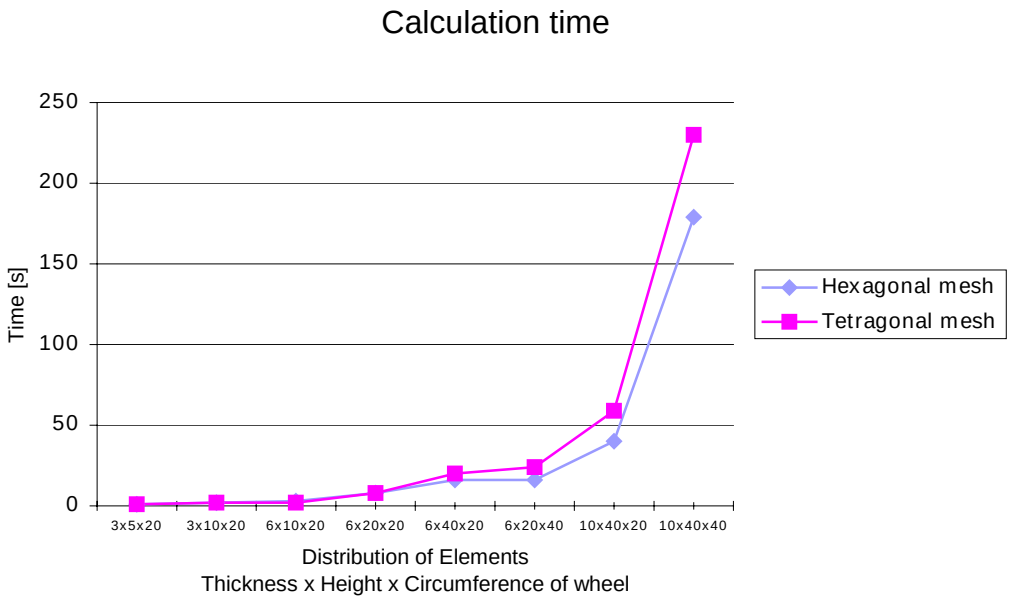

Fig.4. Results of comparison of analytical and numerical calculations - case #3

The analysis shows that the minimum number of elements along the lateral cross-section of the wheel mesh should be equal to six.

These investigations have led to generating an optimum mesh for the mesh with respect to computation accuracy and time

2.2. Subject of investigation – wheel design of railway wheelset

The work was principally aimed at elaborating methods of selection of constructional parameters for the railway wheelset wheels. The conducted calculations of railway wheelsets strains should improve the accuracy of presently used numerical methods and should also be helpful in working out the guidelines for designers, since the calculation algorithm and FEM software are determined.

The numerical investigation has been run for ten different geometrical designs of wheels Ø 920 and Ø 920 – h (worn out), differing by geometrical parameters of the mesh, hub and wheel seat diameter. The generated FE mesh for these wheels has been shown in Fig.5

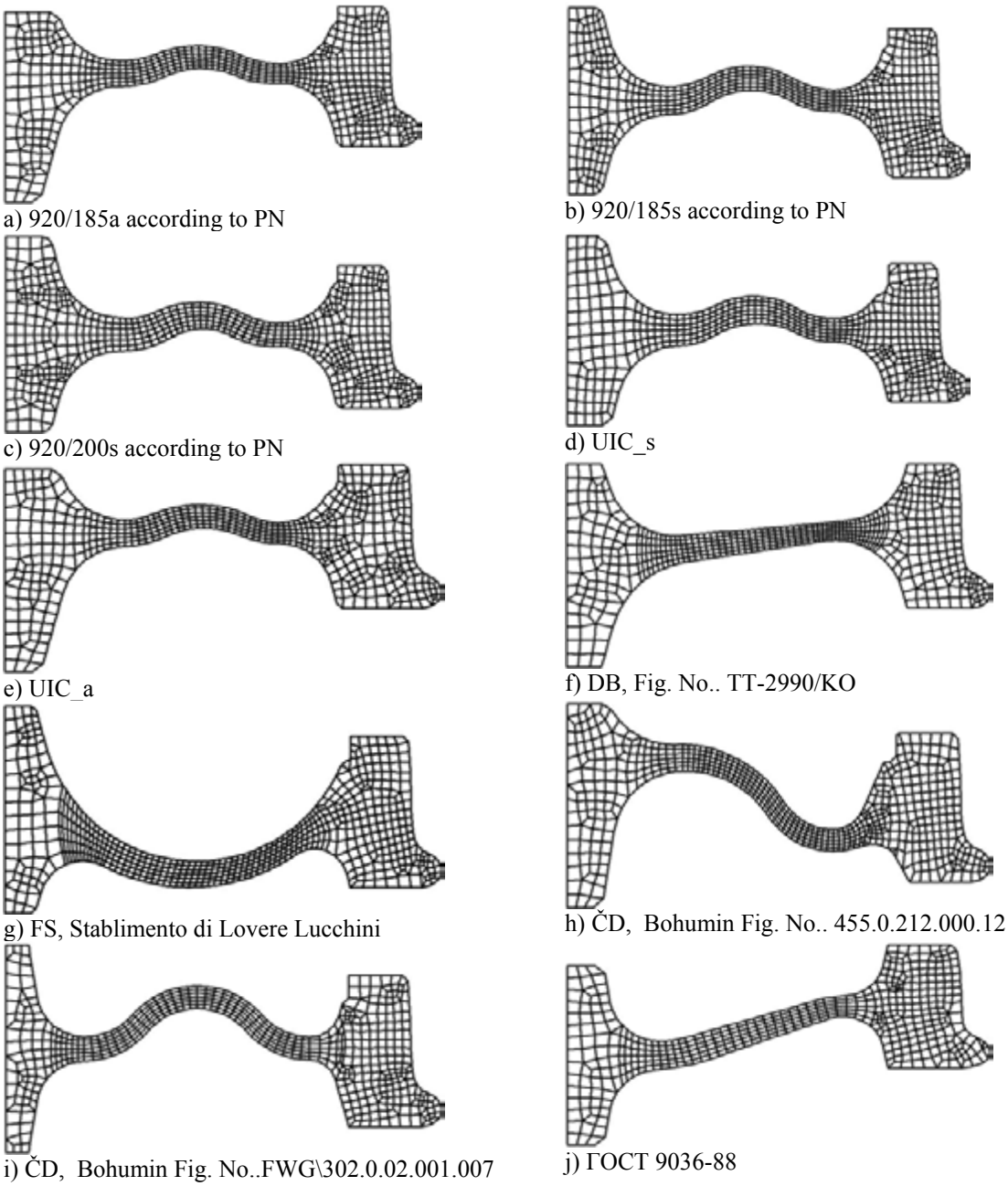

a) 920/185a according to PN
b) 920/185s according to PN
c) 920/200s according to PN
d) UIC_s
e) UIC_a
f) DB, Fig. No.. TT-2990/KO
g) FS, Stablimento di Lovere Lucchini
h) ČD, Bohumin Fig. No.. 455.0.212.000.12
i) ČD, Bohumin Fig. No..FWG\302.0.02.001.007
j) ГОСТ 9036-88

Fig. 5. Discrete models of the investigated monoblock wheels

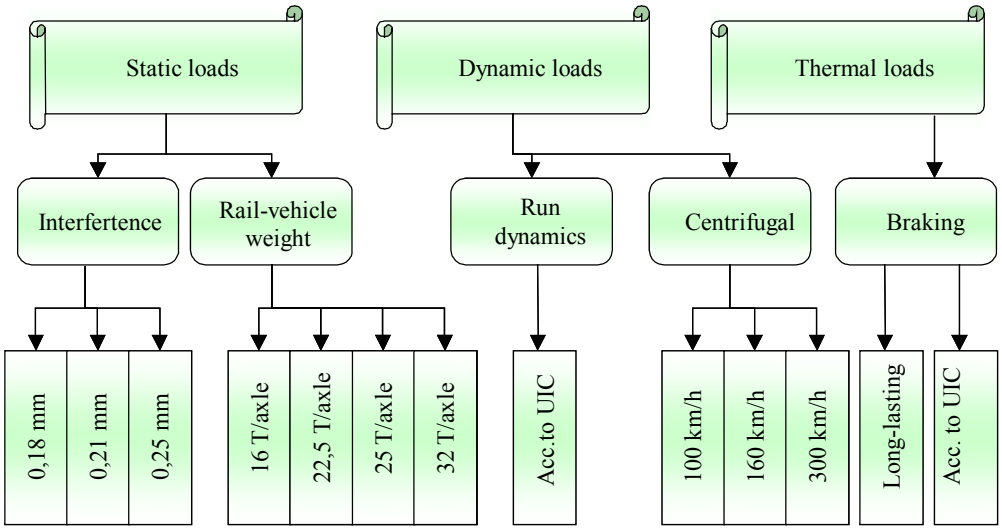

Fig. 6. Wheel loads of the railway wheelset

Next, assembly loads and service loads of the railway wheelset wheel have been determined. These have been used in subsequent research – Fig.6. These are static, dynamic and thermal loads. The static loads are due to interferential fit during the assembly and to carriage weight. The dynamic loads are related to the vehicle run over the track and centrifugal forces resulting from run speed. The thermal loads occur in the wheel during braking. The numerical analysis has been conducted for P52 material (R7 according to UIC classification), which is used for railway wheels in Poland. 3.3. Static loads of the railway wheels.

2.3. Static loads of the railway wheels

2.3.1. Loads due to pressing wheel onto axle

At first, loads due to forces arising from pressing wheel onto axle during the manufacturing process have been analysed The percentage distribution of displacements in the wheel and the axle for the minimum and maximum interference value set by the standards (0.18 – 0.25 mm) has been investigated. This kind of investigation should make possible finding out of the proportion of displacements of interacting elements and this in turn should greatly simplify the analysis.

In order to accurately calculate displacements and stresses due to assembly, an asymmetrical model of wheel and axle has been created, with the adequate number of nodes. Next the node pairs have been coupled with equations determining their displacements. Figure 7 shows this model and corresponding equation for “i-j” node pair (3.13):

$$v_i = v_j$$

$$u_i - u_j = \Delta$$

$$1 \cdot v_i - 1 \cdot v_j = 0 \qquad (3.13.)$$

$$1 \cdot u_i - 1 \cdot u_j + v_k = 0$$

$$\Downarrow$$

$$\Delta$$

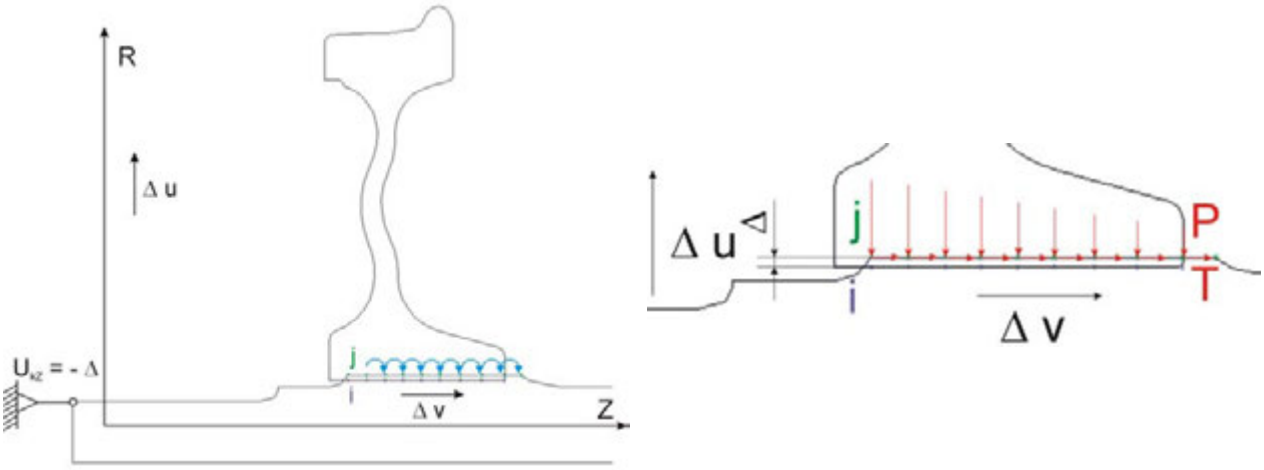

Fig.7. Axially symmetrical load model

$$T = \mu \cdot P$$
$$T_{\Sigma} = \sum_{i=1}^{n} T_i \qquad (3.\ 14.)$$

In order to check the calculation method for the calculated force P value (reaction in the radial direction) and friction coefficient μ determined during pressing tests conducted in Huta Gliwice Steel Plant, the pressing force T has been determined for subsequent calculation phases (3.14) with the contact nodes from i to n, where T_i is the value of the axial force in the node.

These calculations have made possible the creation of the diagram of pressing wheel onto the axle and comparing it with the diagram set down in the Polish Standard. This comparison has confirmed the correctness of the calculation method used – Fig.8. The results of analytical calculations do not exceed the chart range specified by the Polish Standard.

Analysing the generated maps (selected maps of the stresses are given in Fig.9) it is seen that the distribution is mostly affected by the symmetry (or asymmetry) of the wheel hub. In the asymmetrical hub the stresses cumulate in this part of the hub, where mesh is located and the amount of stress diminishes in the opposite direction. The uniform distribution of stresses in the

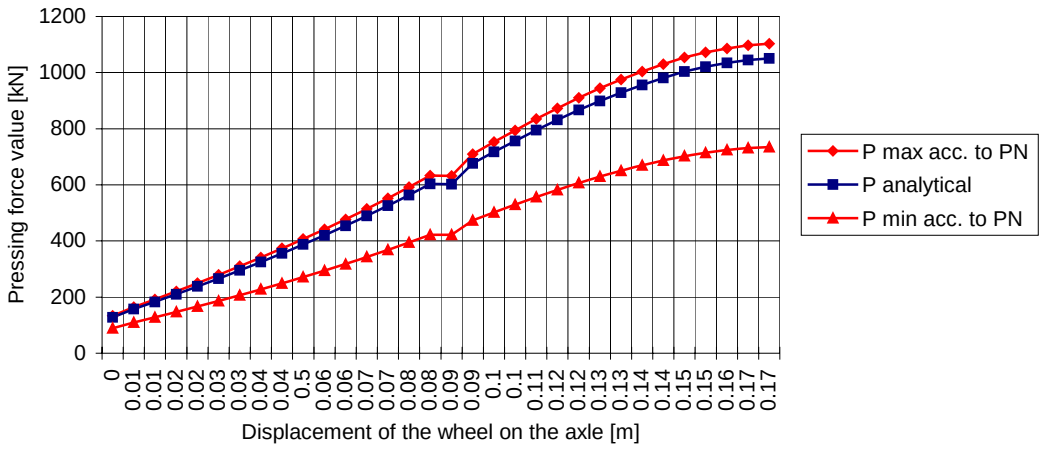

Fig. 8. Theoretical diagram of pressing wheel onto the axle – wheelset PN 920/200s

wheel and the axle characterises wheels with symmetrical hub.

When the wheel is pressed onto the axle, the loads occur also in the places, where the wheel mesh shifts into the hub. It can be concluded from the drawings and calculations, that the less the curvature of the curve joining the mesh to the hub, the less the stress. The use of small radius curves causes accumulation of stress in this particular place.

The calculation of displacements in the wheelset elements has made possible the determination of percentage distribution of contact nodes into the wheelset element. Figure 10 shows the contact nodes displacements in the wheelset for the interference of 0,18 mm. This value seems to be almost independent of the shape of wheel mesh and is equal to 80%. The axle takes up the remaining 20% of the displacement.

The conducted analysis has led to the comparison of the influence of interference value on stress distribution and determination of percentage distribution of interference on different wheelset elements (wheel, axle):

- distribution of the stresses in the wheel does not change (the maximum stresses occur in the wheel hub and mesh bend);
- the stress value changes in proportion to interference value;
- the percentage ratio of the interference transfer is constant for both interference values

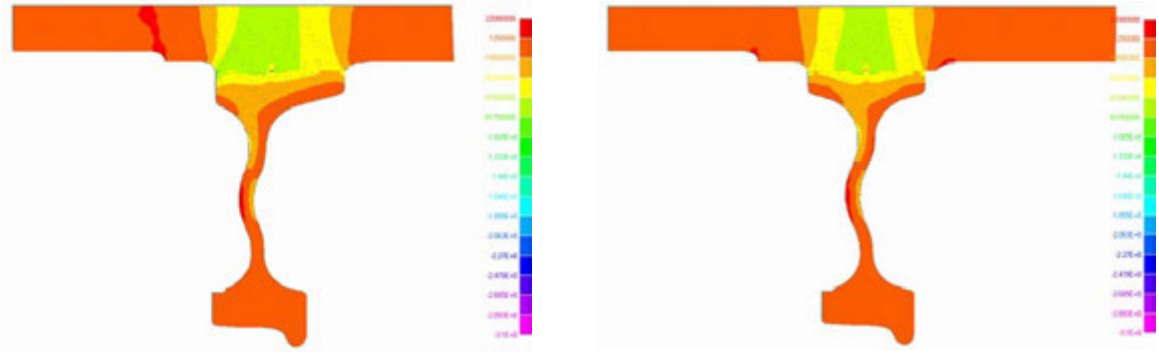

a) 920/185a acc.to PN b) 920/185s acc.to PN

Fig.9. Maps of radial stress of new wheels analysed with axial-symmetrical method for 0.18 mm interference. NASTRAN software

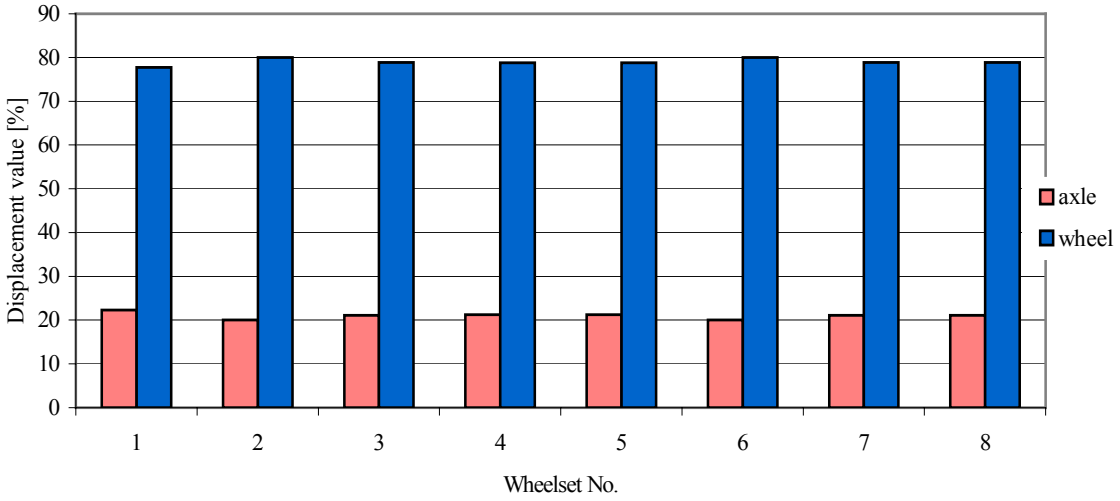

Fig. 10. Displacement of contact nodes in the wheelset

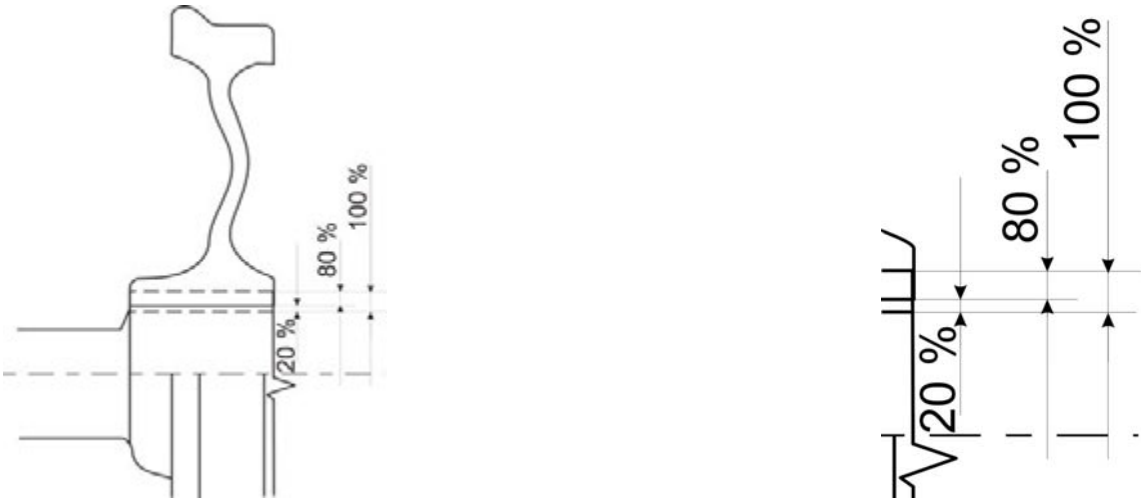

Fig. 11. The percentage ratio of the transfer of interference value for the wheelset elements.

Next, a simplified analysis of the interference has been conducted. Initial linear displacements of the nodes of inner generator surface generator parallel to the radial axis of the global polar co-ordinate system have been defined.

The distribution of stress in both methods has been similar, and the difference in the stress values has not exceeded 10 per cent.

The finding out of the constant proportion of the displacements (i.e. independent of wheel geometry) has made possible the following:

- defining the load caused by pressing wheel onto the axle by the initial displacements;
- shortening of model definition time;
- decreasing the computation time.

Further calculations will be simplified, by setting a pre-determined percentage value of the interference of the element of the railway wheelset – Fig. 11.

Additionally, some calculations have been run for the stresses due to pressing wheel onto the axle for the interference value used in Huta Gliwice Steel Plant and equal to 0,21 mm, for ten different wheel designs (the selected designs have been shown in Fig.12). The analysis has not proven any significant influence of the wheel geometry on the stress value (mesh geometry, the wear of wheel rolling surface). The impact of hub symmetry (or asymmetry) is great. In the case of asymmetrical hub, the stresses cumulate in this part of the hub, where wheel mesh is located and they diminish in the opposite direction. The uniform distribution of stresses in the wheel and axle characterises wheel with symmetrical hub.

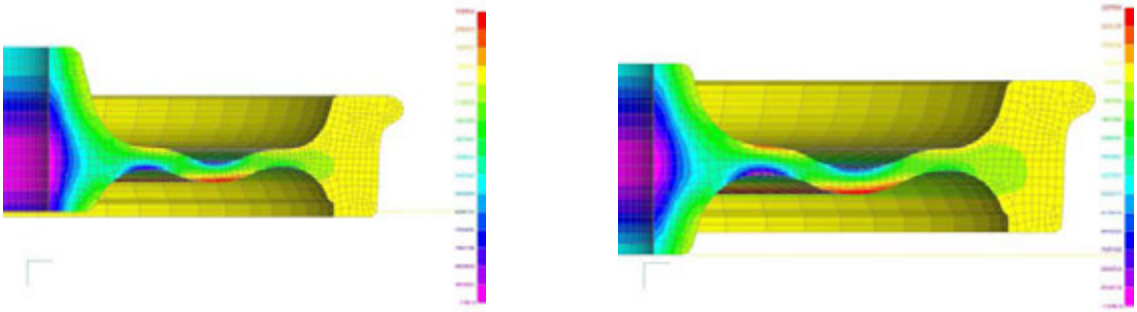

a) 920/185a acc. to PN

b) 920/185s acc. to PN

Fig. 12. Maps of radial stress of wheels analysed with displacement method for 0.18 mm interference. NASTRAN software

2.3.2. Calculations simulating carriage weight

Forces arising from carriage weight constitute another static load. The value and point of application of these forces have been modelled according to UIC guidelines set out in ERI Report B169.1 of 1998 [6].

Axle load of 22,5T per axle is the maximum load set down by Polish Standard for freight carriages. The analysis of maximum reduced stresses caused by the carriage weight has indicated wheels better adapted for carrying huge freights. It is obvious that the most advantageous results for monoblock wheels have been obtained for Russian wheels, since the wheel diameter is greater. However, this type of wheel has achieved the best results in case of maximum wear as well. Good results as to the yield point have been obtained by Polish wheels, UIC symmetrical wheels as well as Italian and Czech wheels (455.0.212). Locations of maximum stresses are similar for different wheel geometries; they occur at the bend connecting the wheel hub with its mesh at both sides. The wear of the rolling surface of the wheel does not have a great impact on the value and distribution of the stress (geometry example is given in Fig. 13).

2.4. Dynamic loads of railway wheels

2.4.1. Loads due to run dynamics

Where run dynamics is in question, UIC guidelines have been followed. The loads have been modelled in a quasi-static way, with a huge safety margin defined by the coefficient [6].

The values of these stress are three times greater than stresses due to carriage weight, the distribution is similar. The wear of the rolling surface of the wheel does not have a great impact on the value and distribution of these stresses.

2.4.2. Loads due to centrifugal forces

Centrifugal forces have been modelled as the speed of the wheel rotating round z-axis. Depending on software used, the units are rpm or rad/s.

In relation to stress generated by other loads these stresses are very small. They can be neglected in further calculation for wheelsets running at normal run speeds (up to 160 km/h).

In case of this type of load the best results have been obtained for Czech wheel Fig. No. FWG\302.0.02.001.007 and Italian wheel. The maximum stress for every analysed design is centred in the wheel mesh. As before, the wear of the rolling surface of the wheel does not have a great impact on the value and distribution of these stresses

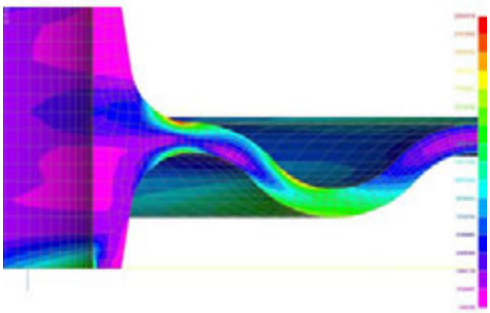

a) ČD, Bohumin Fig. No. .FWG\302.0.02.001.007

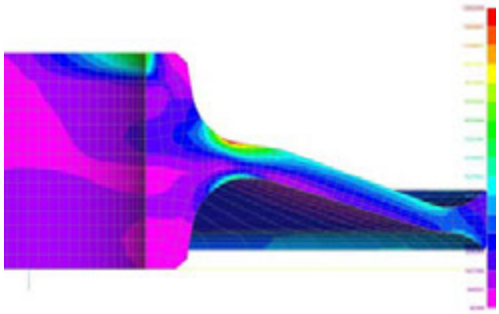

b) ГОСТ 9036-88

Fig. 13. Maps of reduced stresses due to carriage weight, axle load 22,5 T per axle. NASTRAN software

2.5. Thermal loads of railway wheels
2.5.1. Loads due to prolonged braking

The last type of load in question is braking. During analysis, an extreme case of prolonged braking has been modelled (identical to braking taking place in Gotthard Pass [7]). The length of this route is c. 30 km with the average slope of 20,7 and maximum slope of 27‰. Figure 14 shows the convection zones and way of clamping the brake shoe.

The convection values and material properties have been taken from ERI Report 169 of 1987. This report describes investigation of different cases of braking UIC wheel, axle load of 22,5T per axle, at the run speed of 60 km/h (wind puff 0.6* run speed) and braking power of 30 kW. The braking time was 2700 s. During the analysis it has been assumed that 70% of the braking power is transferred to the wheel and the remaining 30 % is absorbed by the brake shoe. The value of the heat flux for the shoe 9- mm wide has been calculated according to the formula.

Applying the above assumptions, calculations of the railway monoblock wheel have been conducted, simulating a prolonged braking.

As could be expected, the lowest maximum reduced stresses have been obtained for the Russian wheel (greater wheel diameter). However, when identical simulation has been run for the worn wheels, this wheel has been marked as the fifth. The overall good results have been obtained by modern-design wheels, with a considerable mesh bend: Italian wheel and Czech wheels (455.0.212 and 302.0.02.001.007). The wheel designed by Stablimento di Lovere Lucchini has shown the best results for the wheel with maximum wear of the rolling surface.

The maximum stresses have always accumulated in the wheel mesh bends.

In case of stresses due to braking, the impact of the wear of the rolling surface on the wheel strength has been observed. In extreme cases the difference in the maximum reduced stresses has been as high as 14 per cent (German wheel TT-2990/KO).

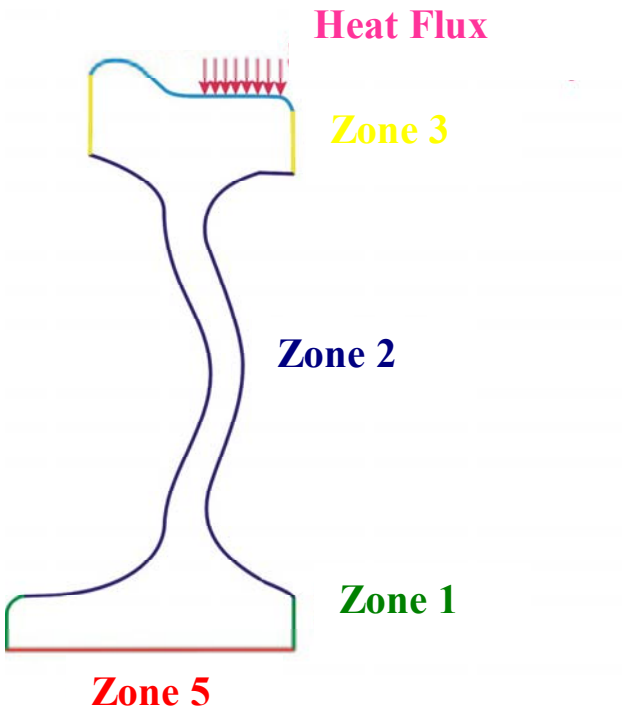

Fig. 14. Modelling thermal loads due to prolonged braking

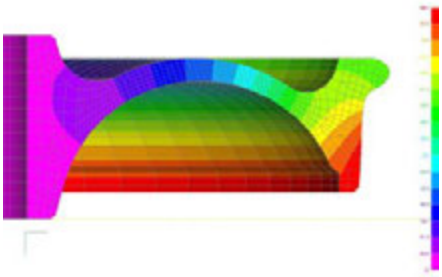

a) FS, Stablimento di Lovere Lucchini

b) ČD, Bohumin Fig. No.. 455.0.212.000.12

Fig. 15. Temperature distribution maps – results of simulation of prolonged braking. NASTRAN software

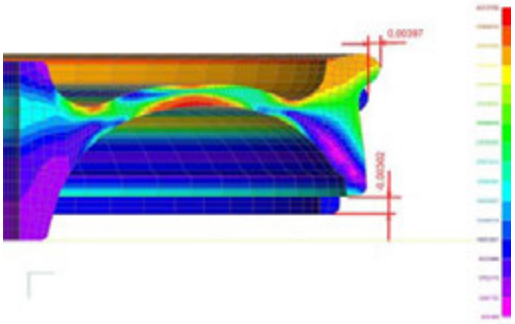

a) FS, Stablimento di Lovere Lucchini

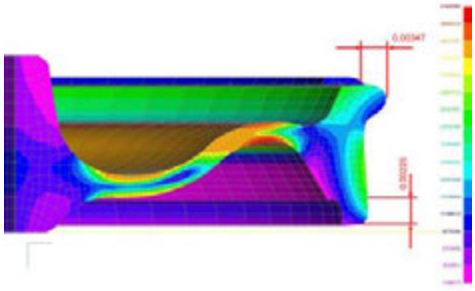

b) ČD, Bohumin Fig. No. 455.0.212.000.12

Fig. 16. Maps of reduced stresses – results of simulation of prolonged braking. Geometry of maximum displacements in both directions has been shown as well. NASTRAN software

2.6. Stress superposition

After the numerical calculations of the several stresses, the superposition of these stresses has been conducted for all the wheels, in accordance with the Polish Standard: PN-92/K-91019: Wagony. Koła Bezobręczowe. Typy i Wymiary (Carriages. Ringless Wheels. Types and Sizes).

The stress distribution has been shown for a Polish wheel PN 920/200s – Fig. 17. The concentration of stresses in this part of the mesh suggests that the decisive impact in the superposition is born by dynamic stresses and stresses due to braking.

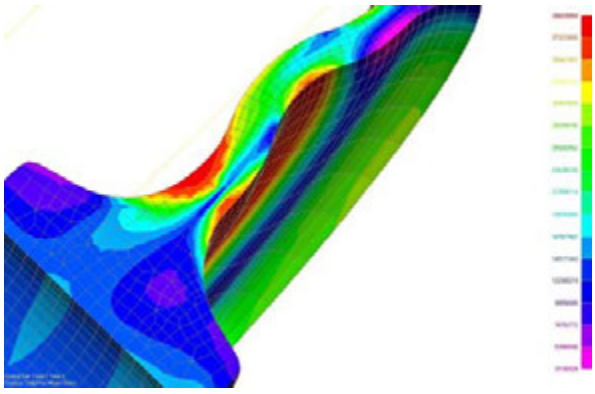

Fig.17. Stress superposition for PN 920/200s wheel

3. THE INFLUENCE OF DESIGN AND SERVICE PARAMETERS ON THE STRESS DISTRIBUTION ON THE RAILWAY WHEEL

3.1. Impact of the mesh geometry

The numerical analysis has demonstrated an insignificant influence of the mesh of wheel geometry on the distribution and values of stresses in case of assembly and static stresses (carriage weight).

When the wheel is pressed onto the axle, the stresses occur in the place, where mesh of the wheel connects to the hub. It can be concluded from the drawings and calculations, that the smaller the curvature of the curve where mesh is joined to the hub, the smaller the stresses. Using small radius curves leads to stress accumulation in these places.

Places, where maximum stresses occur for loads caused by carriage weight are similar for all wheel geometries and are localised at the curve connecting mesh of a wheel to the hub, at both sides. It is obvious that the best results for the monoblock wheel have been obtained for the Russian wheel, since the wheel diameter is greater. However, this wheel has also achieved the best result in case of maximum wear. Good results as to the yield point have been achieved by Polish and UIC wheels (symmetrical) and Italian and Czech wheels (455.0.212). In case of loads due to prolonged braking it has been noted that geometry of the wheel bears a significant impact on the distribution of reduced stresses and, in turn, on the increased wheel strength. The maximum stresses have accumulated in the mesh of a wheel bend. The best results have been obtained by modern-design wheels with a large mesh bend – Italian wheel and Czech wheels (455.0.212 and 302.0.02.001.007). The wheel designed by Stablimento di Lovere Lucchini has generated best results for the wheel with maximum wear of a rolling surface.

The values of the reduced stresses for modern-design wheels have been decreased by 70 MPa (comparison of Italian wheel and UIC asymmetrical wheel, which is widely used – Fig. 18).

3.2. Impact of the wheel hub geometry

In case of symmetry or asymmetry of the mesh of a wheel no noticeable impact on the reduced stress for any load type has been observed. However, change of geometry of the mesh influences the location of stress in case of load due to pressing wheel onto the axle. For the asymmetrical hub, more stress accumulates in this part of the hub, where the mesh is located; the stresses diminish in the opposite direction. Wheels with symmetrical hubs are characterised by uniform distribution of stresses in wheel and axle – Fig.19.

a) b)

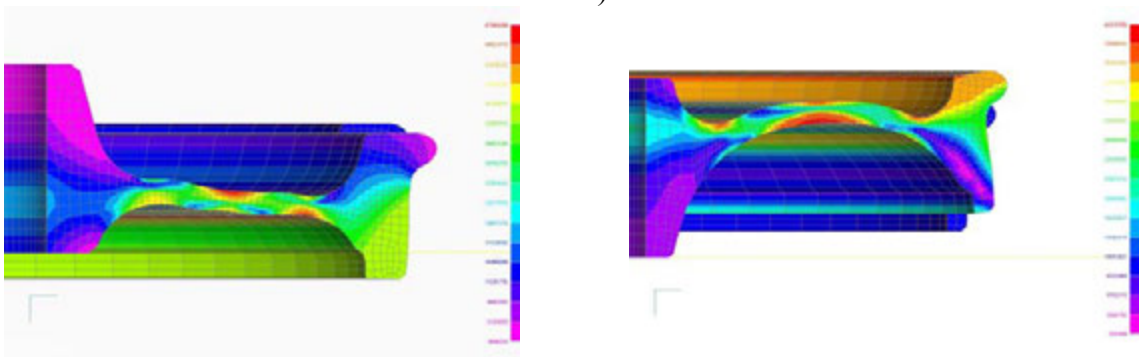

Fig. 18. Comparison of the stress distribution of reduced stresses due to prolonged braking: a) UIC symmetrical wheel, b) Lucchini wheel

a) b)

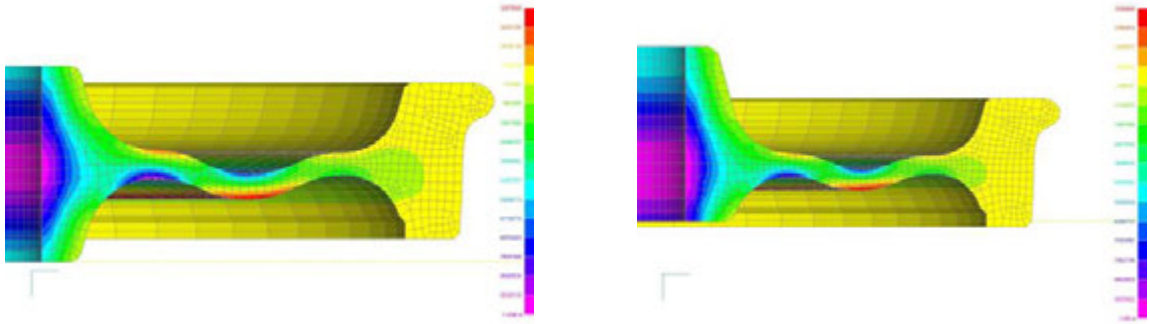

Fig. 19. Distribution of reduced stress caused by pressing wheel onto the axle for wheel in accordance with Polish Standard: a)920/185 symmetrical wheel, b) 920/185 asymmetrical wheel

a) b)

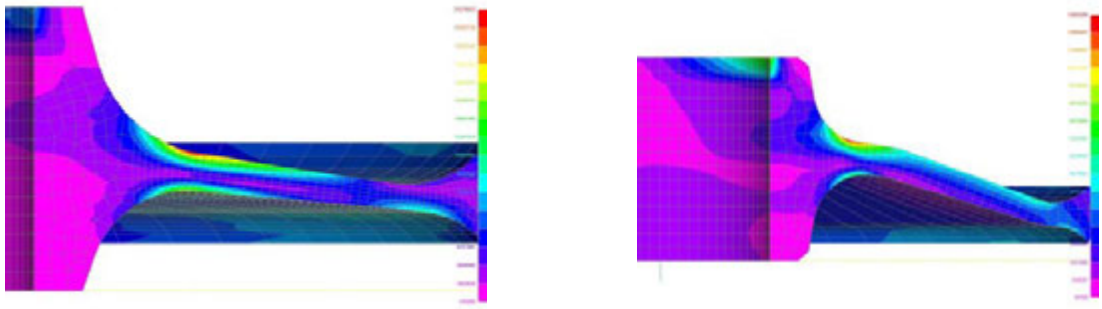

Fig. 20. Reduced stresses due to carriage weight: a) TT2990, b) ГОСТ 9036-88

3.3. Influence of the wheel seat diameter

Significant impact of the wheel seat diameter can be observed in case of the loads due to carriage weight and run dynamics only. The wheels with greater wheel seat diameter (200-267 mm) have generated lower values of the reduced stresses during the numerical analysis. The distribution of the reduced stresses has not changed for all wheel geometries, and stress maximum values are located at the curve connecting wheel hub with mesh of the wheel on both sides – Fig.4.14.

A good example of the influence of wheel seat diameter is the comparison of two wheel types – German wheel (Technical Specification No. TT2990) and Russian wheel – acc. to ГОСТ 9036-88. There is a difference in the wheel seat diameter, while the shape of the mesh is similar. The Russian design is characterised by wheel seat greater by 80 mm (TT2990 = 180 mm, ГОСТ 9036-88 = 263 mm). This design has led to halving the stresses due to static carriage weight and run dynamics – Fig. 20.

3.4. Impact of wheel rolling surface wear

The impact on the wheel strength of the wear of wheel rolling surface has been observed in case of loads due to prolonged braking only (30 kW power, 45 s time interval). The numerical analysis demonstrates the need for investigation and numerical calculations for wheel designs with maximum wear of the rolling surface.In extreme cases the difference in the maximum reduced stresses has been as high as 14 % - German wheel TT-2990/KO – Figure 21.

a) b)

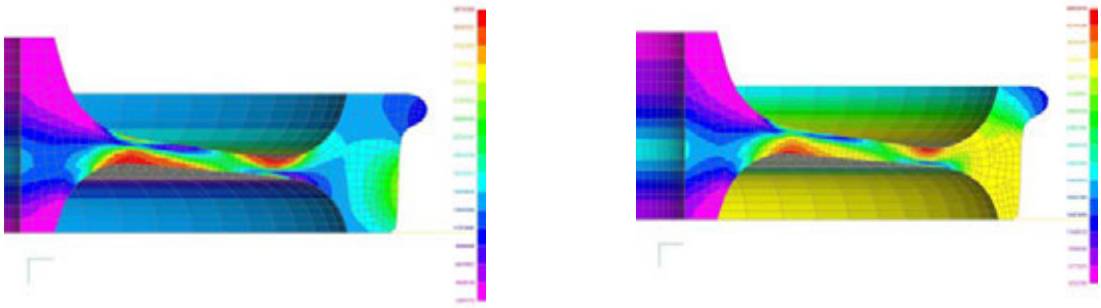

Fig. 21. Distribution of reduced stresses caused by prolonged braking of the German wheel TT2990: a) wheel 920, b) wheel 854

3.5. Summary comparison of ten different designs of railway wheels

In order to indicate the most advantageous design with respect to reduced stresses for given load condition, the wheels with lowest values have been given highest marks (10. Ten different wheel designs). In the same way, inferior wheels received lower marks. The evaluation has been conducted for all load cases, differentiating between new wheels and worn wheels with maximum wear of the rolling surface – Tables 3 and 4.

The marks have been added up in order to select the best design in service.

Table 3. New wheel diameter 920 mm.

Type of wheel	Load type				
	Interference	Carriage weight	Centrifugal forces	Prolonged braking	Total
920/200s	7	9	1	4	**21**
920/185s	3	2	4	3	**12**
920/185a	3	3	1	1	**8**
TT-2990/KO	5	4	4	6	**19**
Lucchini	8	6	9	7	**30**
Bohumin 455.0.212	9	7	7	9	**32**
UIC_s	1	8	4	5	**18**
UIC_a	2	5	1	2	**10**
Bohumin 302.0.02.001.007	9	1	10	8	**28**

Table 4. Wheel with worn rolling surface diameter 854 mm.

Type of wheel	Load type				
	Interference	Carriage weight	Centrifugal forces	Prolonged braking	Total
920/200s	7	8	3	6	**24**
920/185s	4	1	3	4	**12**
920/185a	3	2	1	2	**8**
TT-2990/KO	5	4	3	3	**15**
Lucchini	8	6	9	9	**32**
Bohumin 455.0.212	9	7	7	8	**31**
UIC_s	1	9	3	9	**22**
UIC_a	2	5	1	1	**9**
Bohumin 302.0.02.001.007	10	3	10	7	**30**
ГОСТ9036-88	6	10	7	5	**28**

The best results have been achieved by Czech wheels (455.0.212 and 302.0.02.001.007) and Italian wheel.

Taking into account that these are wheels of modern design (still in the design stages or testing stage), it is important to conduct the numerical analyses and investigations, since these new designs may avail real financial advantages, and increase the safety and travel comfort of future high speed rail vehicles.

4. REMARKS AND CONCLUSIONS

After the numerical analysis of ten different wheel designs has been conducted with the help of three FEM software packages, the obtained results of reduced stress have been compared with respect to: mesh type and pattern, value-dependent stress distribution, wheel construction, degree of wear, used software.

The following conclusions may be drawn:

- mesh type and pattern have great impact on the temperature, displacement and stress fields values;
- geometry of the wheel mesh and hub bear influence on the distribution and values of the stresses. If the service conditions are known, the appropriate wheel geometry can be selected;
- analysis of the degree of wear of the wheel on the distribution and values of the stresses has shown that the influence is significant only in case of loads due to braking;
- comparison of software used has shown significant differences in computation of temperature field caused by braking;
- the conducted analysis has clearly demonstrated the importance of a correct FEM model;
- numerical analysis has made possible comparison o software used in calculations.

The conducted analysis has shown the supremacy of modern-design wheels with respect to the mechanical strength (Italian wheel. Czech wheels 455.0.212 and302.0.02.001.007).

Table 5. Comparison of software used in strain analysis of railway wheelsets

Parameter	Method		
	NASTRAN	ANSYS	COSMOS
1. Facility of data preparation			
• creation of mesh	+/-	+	+/-
• input of material data	+	+	+
• time-consumption	+/-	+/-	+/-
• dependence on temperature	+	+	+
• setting boundary conditions in displacements	+	+	+
• setting loads	+/-	+/-	+/-
2. Rime consumption of:			
• data preparation	+/-	+/-	+/-
• computation	+	+/-	+/-
• results visualisation	+	+	+
3. File import	+	+/-	+/-
4. Contact issues	+	+	+
5. Static issues	+	+	+
6. Dynamic issues	+	+	+
7. Nonstationary heat flow	-	+	+
8. Thermal stresses for a given temperature field	+	+	+
9. Thermal stress issues due to braking	+	+	+
• time consumption	+/-	+/-	+/-
10. Facility of accounting for assembly stresses (interference)	-	-	-
11. Facility of accounting for centrifugal forces	+	+	+
12. Simple wear analysis	-	-	+
13. Superposition of stresses and displacements	+	+	+

REFERENCES

1 **Gąsowski W.**: Wagony kolejowe. Warszawa: WKŁ, 1988

2 **Podemski J., Marczewski R., Majchrzak Z.**: Zestawy kołowe i maźnice. Warszawa: WKiŁ, 1978

3 Materiały Seminarium Szkoleniowego Problemy mechaniki w transporcie szynowym ze szczególnym uwzględnieniem kolejowych zestawów kołowych, TRANSMEC, 05-09 lipiec 2003

4 **Fermer M.**: Optymization of a railway Freight car wheel by use of a fractional design method. Division of Solid Mechanics, Chelmers University of Technology, Goteborg Sweden 2000

5 **Есаулов В.П., Сладковский А.В.**: К расчету напряженного состояния дисков колес, Известия ВУЗов. Машиностроение, 1989, Nr 12, p. 98-103

6 **Raport ERRI B169.1.** Entwurf zum UIC-merkblatt. 1998

7 **Raport ERRI B 169.** Termische grenzen der raden und bremsklotze. MTEL P 98005, Utrecht 198